AD_____
(Leave blank)

Award Number: **W81XWH-12-1-0317**

TITLE: **Targeting Phosphatidylserine for Radioimmunotherapy of Breast Cancer Brain Metastasis**

PRINCIPAL INVESTIGATOR: **Dawen Zhao, M.D., Ph.D.**

CONTRACTING ORGANIZATION: **University of Texas Southwestern Medical Center at Dallas**
Dallas, TX 75390-9058

REPORT DATE: **October 2013**

TYPE OF REPORT: **Annual**

PREPARED FOR: U.S. Army Medical Research and Materiel Command
Fort Detrick, Maryland 21702-5012

DISTRIBUTION STATEMENT: (Check one)

X Approved for public release; distribution unlimited

The views, opinions and/or findings contained in this report are those of the author(s) and should not be construed as an official Department of the Army position, policy or decision unless so designated by other documentation.

REPORT DOCUMENTATION PAGE

Form Approved
OMB No. 074-0188

1. Agency Use Only (Leave blank)	2. Report Date	3. Report Type and Period Covered (i.e., annual 1 Jun 00 - 31 May 01)
	October 2013	Annual,30 September 2012- 29 September 2013

4. Title and Subtitle
Targeting Phosphatidylserine for Radioimmunotherapy of Breast Cancer Brain Metastasis

5. Award Number
W81XWH-12-1-0317

6. Author(s)
Dawen Zhao, M.D., Ph.D.

E-mail: dawen.zhao@UTSouthwestern.edu

7. Performing Organization Name (Include Name, City, State, Zip Code and Email for Principal Investigator)
University of Texas Southwestern Medical Center at Dallas
5323 Harry Hines Blvd.
Dallas, TX 75390-9058

8. Performing Organization Report Number (Leave Blank)

9. Sponsoring/Monitoring Agency Name and Address
U.S. Army Medical Research and Materiel Command
Fort Detrick, Maryland 21702-5012

10. Sponsoring/Monitoring Agency Report Number (Leave Blank)

11. Supplementary Notes (i.e., report contains color photos, report contains appendix in non-print form, etc.)

12a. Distribution/Availability Statement (check one)
X Approved for public release; distribution unlimited

12b. Distribution Code
(Leave Blank)

13. Abstract *(Maximum 200 Words)* *(abstract should contain no proprietary or confidential information)*

Brain metastasis occurs in ~30% of metastatic breast cancer patients. The prognosis is extremely poor, with a median survival of 4-6 months even with aggressive treatment. Thus, there is an urgent need to develop new treatments that target brain metastases. Radioimmunotherapy (RIT) is a targeted therapy that uses radiolabeled antibodies against tumor-specific antigens to treat lymphoma patients. However, success of RIT in the therapy of solid tumors has generally been limited due to heterogeneous tumor expression of the target antigens and cross-reactivity with normal cells. In preliminary studies, we have demonstrated that phosphatidylserine (PS) is exposed exclusively on tumor vascular endothelium of brain metastases in mouse models. A novel PS-targeting antibody, PGN635, a fully human monoclonal antibody, was used to target exposed PS in the brain metastases. Our data show that PGN635 binds specifically to tumor vascular endothelial cells in multi-focal brain metastases throughout the whole mouse brain. Vascular endothelium in normal brain tissues is negative. Furthermore, pretreatment with 10Gy of whole brain radiation significantly increased PGN635 binding to tumor vascular endothelial cells and tumor cells by increasing their exposure of PS. Vasculature in irradiated normal brain remained negative for exposed PS.

14. Subject Terms (keywords previously assigned to proposal abstract or terms which apply to this award)	15. Number of Pages (count all pages including appendices) 32
Breast cancer brain metastasis, Phosphatidylserine, Radioimmunotherapy	16. Price Code

17. Security Classification of Report	18. Security Classification of this Page	19. Security Classification of Abstract	20. Limitation of Abstract
Unclassified	Unclassified	Unclassified	Unlimited

NSN 7540-01-280-5500

Standard Form 298 (Rev. 2-89)
Prescribed by ANSI Std. Z39-18
298-102

Table of Contents

Introduction:

Brain metastasis occurs in ~20% of patients with breast cancer. The prognosis is extremely poor, with a median survival of 4-6 months no matter how aggressive treatment the patients received (1, 2). The incidence of brain metastasis seems to have increased over the past decade. Perhaps even more alarming are the growing numbers of breast cancer patients who die from complications related to brain metastasis, at a time when systemic disease is under good control (3-5). The majority of brain metastases patients exhibit multiple tumors at the time of diagnosis. Even in the event of a solitary metastasis, it is believed that the entire brain can be seeded with many radiographically invisible metastases. Due to the high incidence of multiple brain lesions and the limited leakage of most chemotherapeutics through blood brain barrier (BBB), the standard care for these patients is whole brain radiotherapy (WBRT). WBRT, however, is often associated with neurological complications that preclude sufficient doses delivered to tumor lesions (2, 6). Thus, there is an urgent need to develop new treatment regimens against the devastating disease.

Monoclonal antibody-based therapies, *i.e.*, anti-Her2 trastuzumab, are demonstrating clinical efficacy in treating primary breast cancer (7). However, inability to cross BBB limits their application for treatment of brain metastases. Radioimmunotherapy (RIT), by linking antibodies with radioisotopes, enhances tumor cytotoxicity by directly killing antibody-binding tumor cells or killing neighboring tumor cells by crossfire effect (8, 9). RIT thus offers an opportunity to selectively radiate tumor cells while sparing normal tissues. The high energy β^- emitter, Yttrium-90 (^{90}Y), a FDA approved radiotherapeutic, has been successfully used clinically to treat Non-Hodgkin's lymphomas (10, 11). However, success of RIT in the therapy of solid tumors has generally been limited due to heterogeneous tumor expression of the target antigens and cross-reactivity with normal cells.

Our preliminary studies have found that phosphatidylserine (PS) is exposed extensively on tumor vascular endothelium of brain metastases, but not blood vessels of normal brain in a mouse model of breast cancer brain metastasis (12). A novel PS-targeting, fully human antibody, PGN635, has been applied and showed a great sensitivity and specificity of binding exposed PS in these brain metastases. Furthermore, pretreatment with low dose of whole brain radiation significantly increased PGN635 binding to tumor vascular endothelial cells and tumor cells by increasing their exposure of PS. Given it's specifically for tumor vasculature and the lack of a need to cross the BBB, we propose to apply PGN635 RIT to treat brain metastasis of breast cancer in mouse models. We further hypothesize that RIT in combination with low dose WBRT will not only achieve effective treatment of brain metastases but also minimize the side effects.

Because PS is the same molecule and has the same distribution and regulation in all mammalian species, it is likely that the mouse data will extrapolate to humans. We believe that successful completion of this project will lay a foundation for clinical development of a novel treatment for breast cancer brain metastasis.

Body:

The Statement of Work in this period had two major tasks:

Task 1. **To study phosphatidylserine (PS) exposure on tumor vasculature and tumor cells of breast cancer brain metastasis mouse models, and determine if exposed PS is increased by radiation.**

a. Establishment of various breast cancer brain metastases mouse models:

The intracardiac model of Breast cancer brain metastasis has been successfully established by ultrasound-guided left ventricle injection of various breast cancer brain seeking cells, including MDA-MB231Br-EGFP, MCF7Br-Her2 (kindly provided by Drs. Palmieri and Steeg) and syngeneic 4T cells.

b. MRI monitoring of intracranial growth of brain metastasis:
Extensive longitudinal MRI studies were conducted to non-invasively monitor the initiation and intracranial development. MRI observed multifocal brain metastases in the MDA-MB231Br (Fig. 1a) model while a solitary metastasis in the MCF7Br-Her2 model (Fig. 1b) and the 4T1 model (Fig. 1c).

a

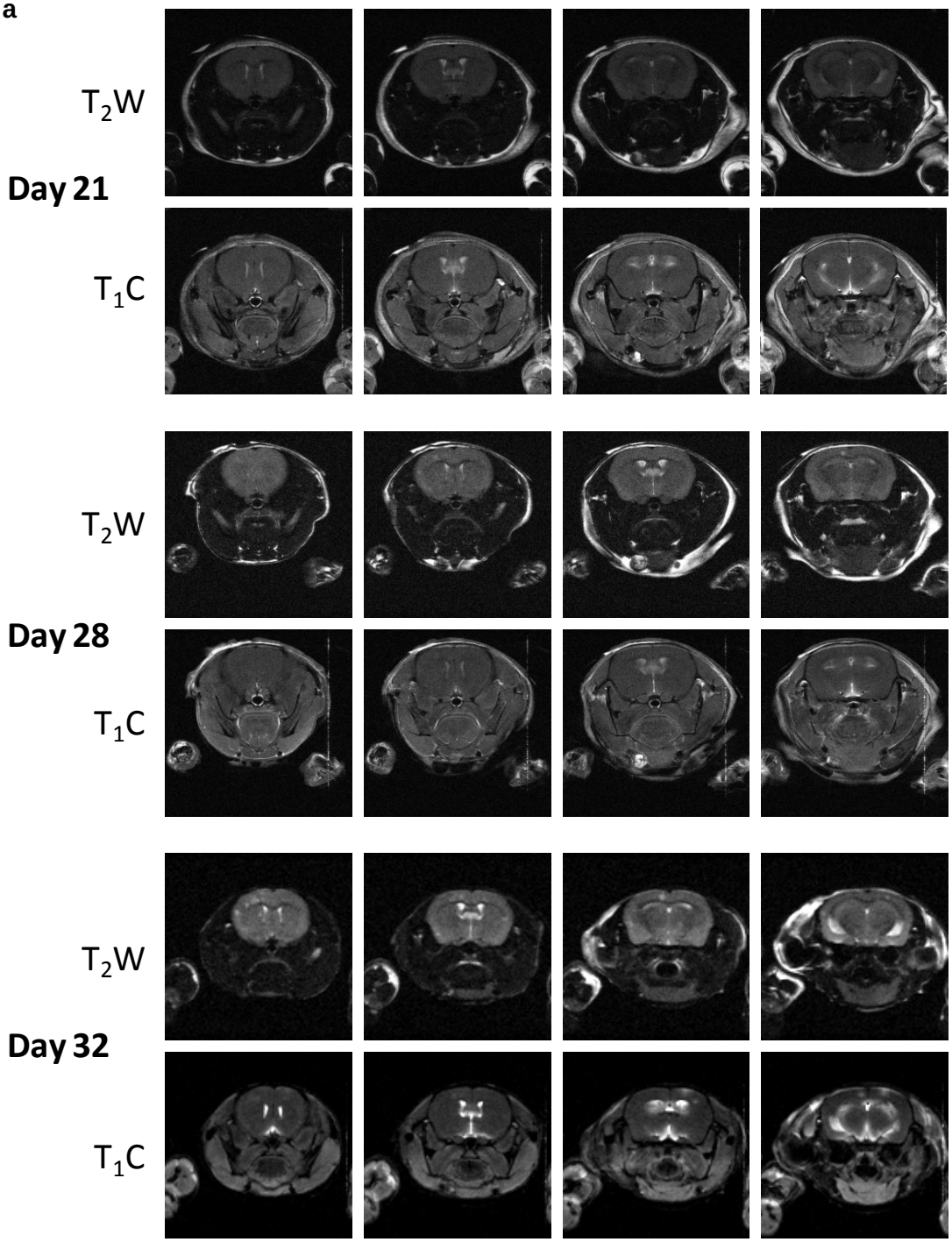

b

c

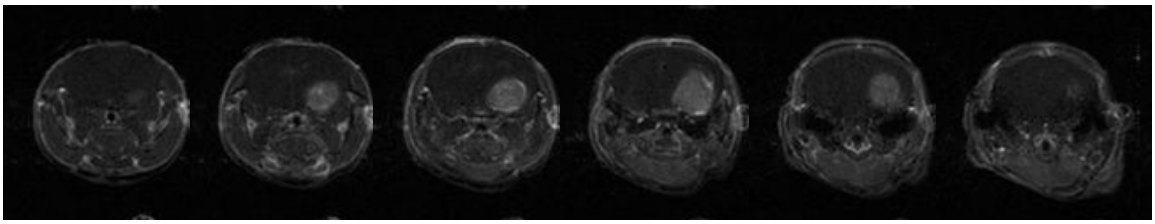

Fig. 1 MRI detection of brain metastases of mouse models. a. Longitudinal MRI monitoring of intracranial development of multifocal brain metastases in the MDA-MB231Br-EGFP model. **b and c.** A solitary brain metastasis was identified for the MCF7Br-Her2 and the 4T1 model, respectively.

c. Detection and quantification of exposed PS. PS exposure on vascular endothelium and tumor cells of brain metastases were quantified based on immunohistochemical staining of PGF635 and co-stained with vascular endothelial marker, CD31 (Fig. 2).

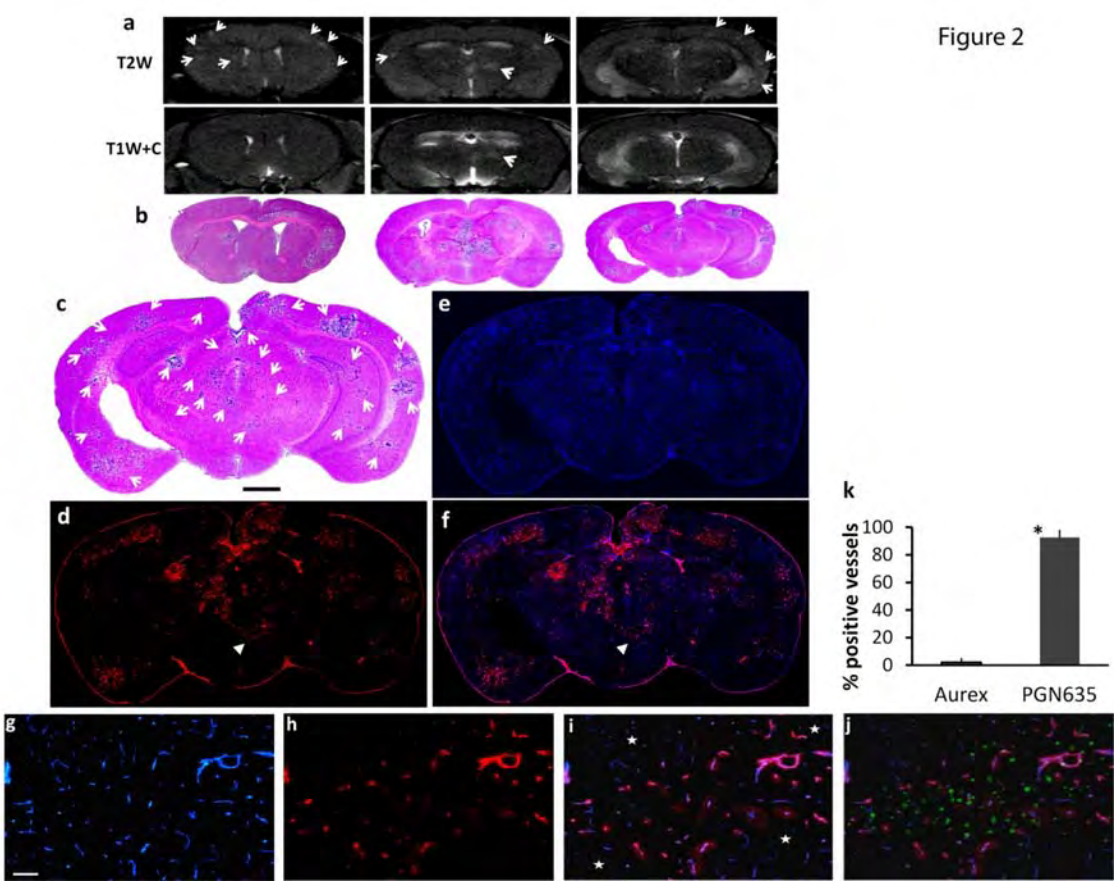

Fig. 2 Staining of PGN635 depicts individual brain metastases. a. 2 x 10^5 MDA-MB-231/BR-GFP cells were injected into the left ventricle of a mouse heart. At week 5, three consecutive coronal sections of high resolution MRI of the mouse brain revealed multiple high signal intensity lesions on T_2-weighted images (arrow), while only a single lesion was enhanced on T_1-weighted post contrast images (arrow). Immediately after MRI, the mouse was injected i.v. with PGN635. Four hour later, the mouse was perfused and the brain was dissected. **b.** Corresponding H&E staining showed a good correlation with MRI. **c-f.** Diffuse lesions were labeled on one of the H&E sections (arrow). Immunofluorescence staining on a consecutive section showed that PGN635 (red; **d**) localized to every tumor lesion, even microscopic lesions identified by H&E staining (arrow; **c**). Binding of PGN635 to tumor vessels (CD31, blue; **e**) was confirmed by the magenta color in merged images (**f**). **g-j.** A region containing positive PGN635 (arrowhead in **d**) was selected and magnified (bar = 100 µm). The merged image showed that PGN635 (red, **h**) co-localized with almost every CD31-positive tumor vessel (blue, **g**) to give a magenta color (**i**). Vessels in nearby normal brain (star, **i**) were not stained by PGN635. The tumor regions were distinguished from normal brain by the presence of GFP in the tumor (**j**). **k.** The percentage of PS-positive vessels in brain metastases was 93 ± 5%., while only 2 ± 2% for the control antibody Aurexis. * $p < 0.01$.

Individual brain metastases of MDA-MB231Br can clearly be depicted simply based on PGN635 staining. Quantitative analysis of PS exposure on vascular endothelial cells of brain metastases revealed 93 ± 5% of tumor vessels had exposed PS. The data suggest that PS is highly specific to tumor vasculature of brain metastases (Fig. 2).

Extensive immunohistochemical studies were also conducted on investigating if tumor hypoxia induces PS exposure on vascular endothelial cells. As presented in Fig. 3, there was no hypoxic region detectable in these individual metastases by pimonidazole staining, indicating other causes than hypoxia may be related to PS exposure.

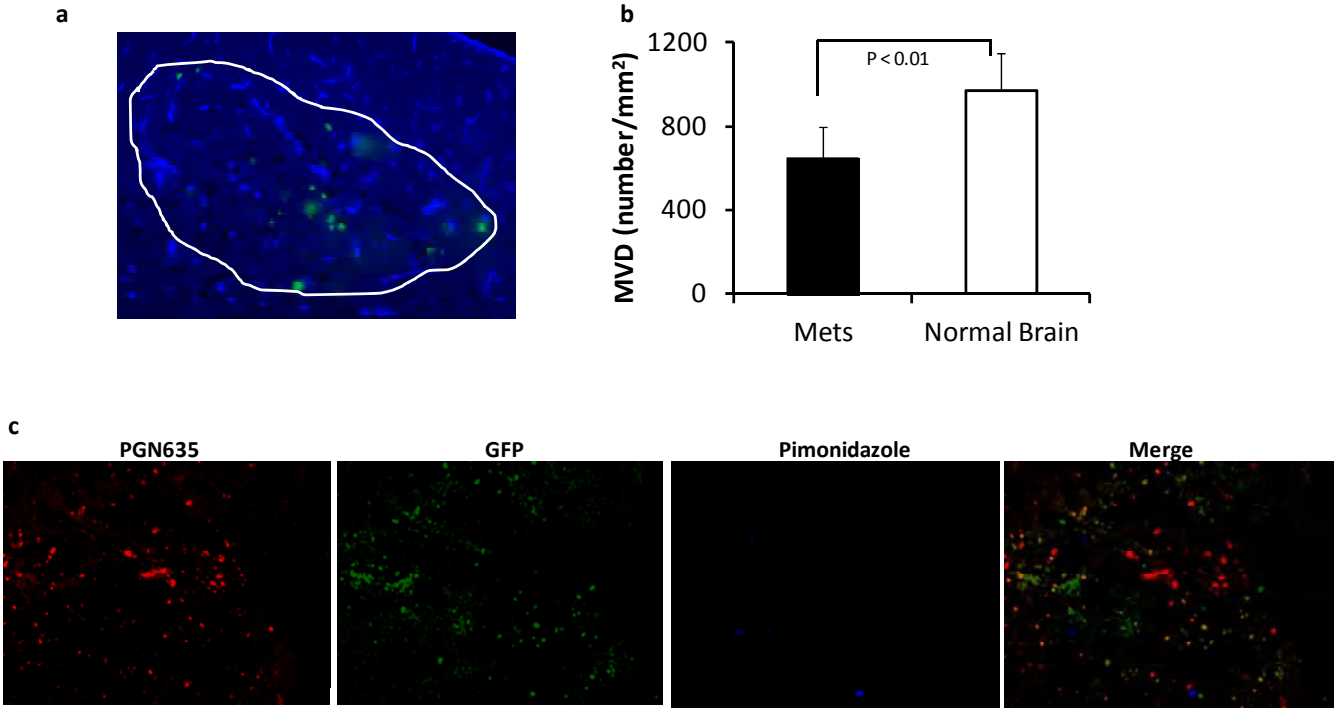

Fig. 3 Immunohistological studies of microvascular density (MVD) and hypoxia in individual metastases of 231-Br model. a. For a representative region bearing a brain metastasis, an outline was drawn based on the green-staining of tumor cells (GFP) to separate the metastatic lesion from surrounding normal brain. Microvessel staining by anti-CD31 (blue) showed less dense MVD within the brain metastasis, as compared to the outside normal brain. **b.** Statistic analysis indicated a significantly lower MVD in brain metastases (mean = 646 ± 149) than that of surrounding normal brain (972 ±177; $p < 0.01$). **c.** Pimonidazole staining detected essentially no tumor hypoxia in brain metastases.

d. Detection and quantification of exposed PS after whole brain radiation.
Irradiation studies are undergoing.

Task 2. **To radiolabel the PS-targeting antibody, mch635, with β^- emitters and evaluate its biodistribution and pharmacokinetics in breast cancer brain metastasis mouse models.**

a. Radiolabel PGN635F(ab')2
b. Evaluate stability and binding specificity *of the radio-conjugates in vitro.*
c. Develop breast cancer brain metastasis with the 4 breast cancer cell lines.
d. MRI monitoring of intracranial growth of brain metastasis.
e. *In vivo* studies of biodistribution and dosimetry in healthy mice and in mice bearing brain metastases.

PGN635F(ab')2 were successfully labeled with I-124 or I-125 to study its specific targeting of brain metastases and biodistribution. The imaging data in Fig.4 indicate the radiolabeled PGN635 can serve as a specific imaging probe for sensitive detection of brain metastases in mice.

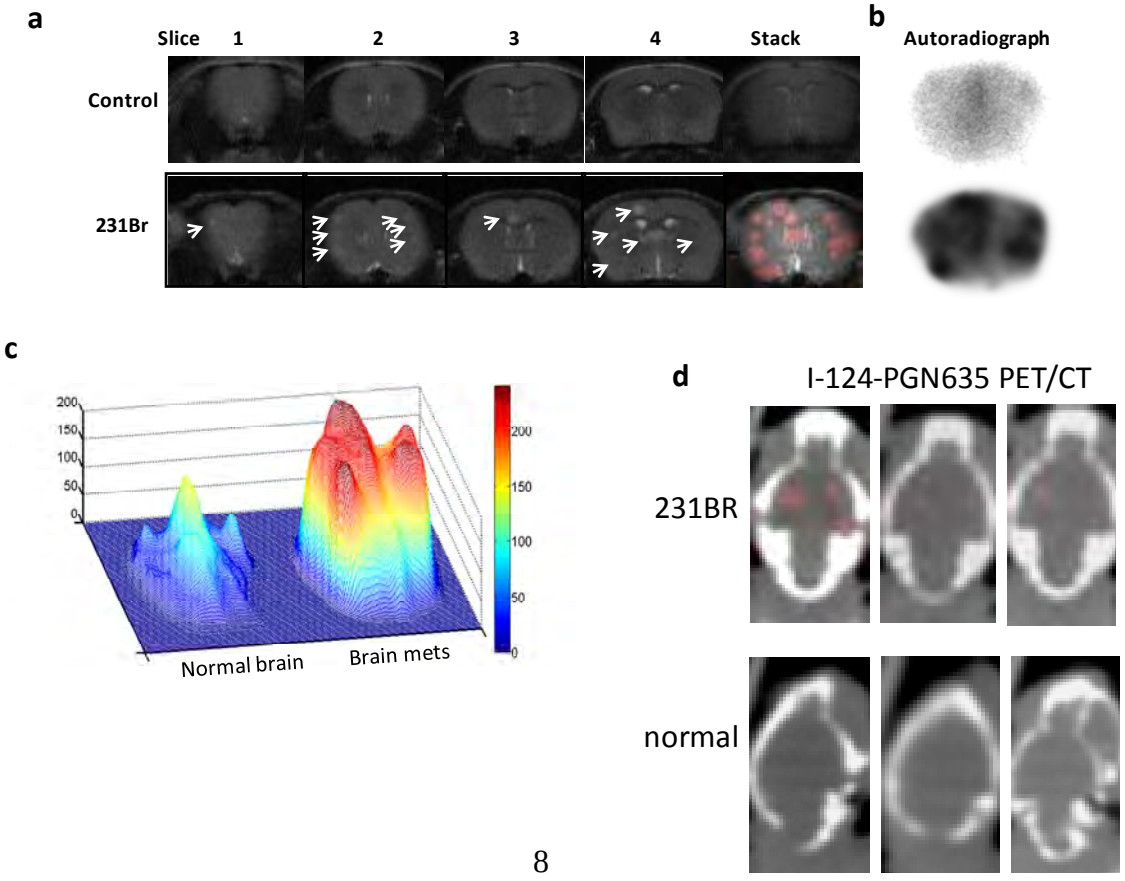

Fig. 4 Autoradiography and PET imaging of I-124/125 labeled PGN635 in targeting brain metastases. a. T_2-weighted MR images of 4 consecutive 1 mm thick coronal slices, covering 4mm brain tissues post bregma, were acquired from a normal control mouse brain (top) and a 231-Br brain (bottom) 40 days after intracardiac injection, respectively. Multiple tumors in the 231Br brain were identified (arrow). The stacked images were created from the 4 slices for each animal. For the tumor brain, the tumor lesions (red) from each slice were projected on the stacked image in order to correlate with autoradiography study. **b.** After MRI, each mouse was given i.v. ^{125}I-PGN635 F(ab')$_2$. Forty-eight hours later, the mice were perfused and mouse brains were dissected. Using a mouse brain matrix, 4mm thick brain tissues post bregma, correlating with the MRI, were cut from each mouse brain and laid the cutting face on the autoradiograph film. After 12 hr incubation, autoradiograph images showed multiple hot spots on the tumor brain, while clean background signal observed on the normal brain. There was also a general spatial correlation between tumor lesions on MRI and hot spots on the autoradiograph. **c.** Significantly higher uptake of ^{125}I-PGN635 was seen in the individual lesions, as compared to normal brain tissues (a ratio of 3.6±0.8; $p < 0.05$). **d.** ^{124}I-PGN635 F(ab')$_2$ (50 µg / 50 µCi) was injected into a MDA-MB231Br mouse via a tail vein. PET/CT images were acquired 24 h (not shown) and 48 h later. PET/CT merged images at 48 h showed multiple localized uptake by the mouse brain, which were highlighted on the 3 consecutive transaxial images, indicating the uptake of ^{124}I-PGN635 by the metastatic lesions. In contrast, there was a complete lack of uptake of ^{124}I-PGN635 in a normal control mouse.

Key Research Accomplishments

- **Establishment of the intracardiac model of breast cancer brain metastasis with various brain-tropic metastatic breast cancer cells including MDA-MB231Br-EGFR, MCF7Br-Her2 and syngeneic 4T1 cells.**

- **Successful application of longitudinal MRI to monitor intracranial metastases distribution, tumor growth and BTB permeability.**

- **Immunohistochemical studies show PS exposure is specifically located on tumor vascular endothelial cells of brain metastases while the normal vessels surrounding the metastases lack of exposed PS, suggesting that PS can serve as a brain metastasis-specific biomarker.**

- **The fragments of PS-targeting antibody, PGN635F(ab')2 have been successfully conjugated with near infrared dye, allowing in vivo and ex vivo optical imaging of clear tumor contrast that enables demarcation of individual metastases from surrounding normal brain tissues.**

- **Immunohistochemical and histological studies of tumor vasculature, PS exposure and tumor hypoxia found no positive staining of tumor hypoxia marker, pimonidazole in individual metastases in the multifocal model of MDA-MB231Br-EGFP, excluding the possibility that tumor hypoxia induces PS exposure on tumor vascular endothelial cells.**

- **Autoradiography and PET imaging of radioactive iodine labeled PGN635 confirmed the targeting specificity of PGN635 and indicate the radiolabeled PGN635 can serve as a specific imaging probe for sensitive detection of brain metastases.**

Technique problem

It is sad that we lost Dr. Thorpe, the Partner PI of this project. Dr. Thorpe passed away in the middle of the first period. The studies proposed in Task 1 c and d and Task 2e were significantly delayed. Fortunately, Dr. Brekken, an expert in antibody development and cancer therapeutics agreed to participate in the project as the Partner PI. We are confident that we are able to make up for the loss and move on.

Reportable Outcomes

Publications:

Peer-reviewed paper:

1. Zhou, H., Chen, M., **Zhao, D**. Longitudinal MRI evaluation of intracranial development and vascular characteristics of breast cancer brain metastases in a mouse model. *PLoS ONE,* 8(4): e62238, 2013.

2. Zhou, H. and **Zhao, D**. Ultrasound imaging-guided intracardiac injection to develop a mouse model of breast cancer brain metastases followed by longitudinal MRI. *J. Vis. Exp.* In press, 2013.

Published Conference Proceedings:

1. **Zhao, D.,** Zhou, H., Stafford, J., Thorpe, P. Targeting phosphatidylserine enables the clear demarcation of brain metastases in mouse models. *Cell Symposium: Hallmarks of Cancer,* P2.028, San Francisco, CA, 2012.

2. **Zhao, D.,** Zhou, H., Stafford, J., Thorpe, P. (**Invited talk**) Imaging of tumor vascular endothelial cells in living mice. *Photonics West of SPIE,* 8596-3, San Francisco, CA, 2013.

3. **Zhao, D.,** Zhou, H., Chiguru, S., Slavine, N., Stafford, J., Thorpe, P. Phosphatidylserine targeted multimodal imaging of brain metastases in mouse models. *World Molecular Imaging Congress*, p591, Savannah, GA, 2013.

4. Zhang, L., Zhou, H., Thorpe, P., **Zhao, D.** *In vivo* MRI and optical imaging of tumor vascular endothelial cells using bimodal liposomal nanoparticles. *World Molecular Imaging Congress*, p263, Savannah, GA, 2013.

Employment or research opportunity:

The PhD student and research assistant, Heling Zhou, has completed her PhD dissertation and was awarded the PhD degree. Dr. Zhou is continuing her research of cancer imaging as a postdoctoral fellow in Radiology Department of UT Southwestern Medical Center.

The Postdoctoral fellow, Liang Zhang, has been recruited to work on this project.

Conclusion:

During the first year of this project, we have successfully established brain metastases mouse models of various brain-tropic breast cancer cell lines. Longitudinal MRI enabled in vivo monitoring of the initiation and growth of individual brain metastases. The high sensitivity and specificity of the novel phosphatidylserine-targeting antibody, PGN635 enables individual metastases, even those micrometastases containing intact BTB to be clearly delineated. Non-invasive imaging of mice injected with PGN635 labeled with IRDye 800CW or ^{124}I-PGN635 allowed clear visualization of individual brain metastases. Given its intravascular localization and the lack of a need to cross the BTB, PS appears to be an excellent marker for the development of imaging and targeted therapeutics for brain metastases.

References:

1. Chang EL, Lo S. Diagnosis and management of central nervous system metastases from breast cancer. Oncologist 2003; 8: 398-410.
2. Gaspar L, Scott C, Rotman M, et al. Recursive partitioning analysis (RPA) of prognostic factors in three Radiation Therapy Oncology Group (RTOG) brain metastases trials. Int J Radiat Oncol Biol Phys 1997; 37: 745-51.
3. Subramanian A, Harris A, Piggott K, Shieff C, Bradford R. Metastasis to and from the central nervous system--the 'relatively protected site'. Lancet Oncol 2002; 3: 498-507.
4. Begley DJ. Delivery of therapeutic agents to the central nervous system: the problems and the possibilities. Pharmacol Ther 2004; 104: 29-45.
5. Doolittle ND, Abrey LE, Bleyer WA, et al. New frontiers in translational research in neuro-oncology and the blood-brain barrier: report of the tenth annual Blood-Brain Barrier Disruption Consortium Meeting. Clin Cancer Res 2005; 11: 421-8.
6. Lutterbach J, Bartelt S, Ostertag C. Long-term survival in patients with brain metastases. J Cancer Res Clin Oncol 2002; 128: 417-25.
7. Carter P. Improving the efficacy of antibody-based cancer therapies. Nat Rev Cancer 2001; 1: 118-29.
8. Ran S, Downes A, Thorpe PE. Increased exposure of anionic phospholipids on the surface of tumor blood vessels. Cancer Res 2002; 62: 6132-40.
9. Ran S, Thorpe PE. Phosphatidylserine is a marker of tumor vasculature and a potential target for cancer imaging and therapy. Int J Radiat Oncol Biol Phys 2002; 54: 1479-84.
10. Emmanouilides C. Review of Y-ibritumomab tiuxetan as first-line consolidation radio-immunotherapy for B-cell follicular non-Hodgkin's lymphoma. Cancer Manag Res 2009; 1: 131-6.
11. Lau WY, Lai EC, Leung TW. Current Role of Selective Internal Irradiation with Yttrium-90 Microspheres in the Management of Hepatocellular Carcinoma: A Systematic Review. Int J Radiat Oncol Biol Phys.
12. Zhao D, Zhou, H., Chiguru, s., Slavine, N., Stafford, J.H., Thorpe, P.E. Targeting Phosphatidylserine enables the clear demarcation of brain metastases in mouse models. *Cell Symposium: Hallmarks of Cancer*; 2012; San Francisco, CA; 2012. p. P2.028.

Appendices

Phosphatidylserine-targeting antibody enables clear imaging of brain metastases in mouse models

Dawen Zhao[1], Heling Zhou[1], Srinivas Chiguru[1], Jason H. Stafford[2], Philip E. Thorpe[2].

Departments of Radiology [1], Pharmacology[2], UT Southwestern Medical Center, Dallas, TX, USA.

Brain metastases are the most common intracranial malignancy in adults. The prognosis is poor partly because most patients diagnosed with a solitary cerebral metastasis have undetected lesions, and current systemic therapies have limited access to occult metastases with an impermeable brain-tumor-barrier (BTB). It has recently been observed that phosphatidylserine (PS) becomes exposed on the outer surface of viable endothelial cells in tumor blood vessels. In this study, we used a fully human monoclonal antibody, PGN635, that targets PS to identify brain metastases in mouse models. Fluorescence microscopy of sections of brain showed that there is extensive PS exposure on vascular endothelial cells in brain metastases but not in normal brain. Non-invasive imaging of mice injected with PGN635 labeled with a near infrared dye allowed clear visualization of individual brain metastases. PS appears to be an excellent marker for the development of imaging and targeted therapeutics for brain metastases.

In vivo imaging of tumor vascular endothelial cells

Dawen Zhao[*], Jason H. Stafford[ϕ], Heling Zhou[*], Philip E. Thorpe[ϕ]

Departments of Radiology [*] and Pharmacology[ϕ], UT Southwestern Medical Center,

Dallas, TX 75390

ABSTRACT

Phosphatidylserine (PS), normally restricted to the inner leaflet of the plasma membrane, becomes exposed on the outer surface of viable (non-apoptotic) endothelial cells in tumor blood vessels, probably in response to oxidative stresses present in the tumor microenvironment. In the present study, we optically imaged exposed PS on tumor vasculature *in vivo* using PGN635, a novel human monoclonal antibody that targets PS. PGN635 F(ab')$_2$ was labeled with the near infrared (NIR) dye, IRDye 800CW. Human glioma U87 cells or breast cancer MDA-MB-231 cells were implanted subcutaneously or orthotopically into nude mice. When the tumors reached ~5 mm in diameter, 800CW-PGN635 was injected via a tail vein and *in vivo* dynamic NIR imaging was performed. For U87 gliomas, NIR imaging allowed clear detection of tumors as early as 4 h later, which improved over time to give a maximal tumor/normal ratio (TNR = 2.9 ± 0.5) 24 h later. Similar results were observed for orthotopic MDA-MB-231 breast tumors. Localization of 800CW-PGN635 to tumors was antigen specific since 800CW-Aurexis, a control probe of irrelevant specificity, did not localize to the tumors, and pre-administration of unlabeled PGN635 blocked the uptake of 800CW-PGN635. Fluorescence microscopy confirmed that 800CW-PGN635 was binding to PS-positive tumor vascular endothelium. Our studies suggest that tumor vasculature can be successfully imaged *in vivo* to provide sensitive tumor detection.

Key Words: Phosphatidylserine (PS), near-infrared (NIR) optical imaging, tumor vasculature, glioma, breast cancer

1. INTRODUCTION

Molecular imaging of angiogenesis has recently been demonstrated using ligands that target biomarkers that are selectively exposed on tumor vasculature. The integrin alpha v beta III ($\alpha v\beta 3$), which is overexpressed on the surface of tumor vascular endothelial cells, has been the most widely used target to imaging tumor angiogenesis. Various imaging contrast agents have been conjugated to $\alpha v\beta 3$ binding ligands, such as Arginine-Glycine-Aspartic Acid (RGD)-containing peptide, for PET, SPECT, MRI and optical imaging (1). Optical imaging is increasingly being used in preclinical cancer research. It is being used to study cancer specific markers, drug pharmacokinetics, and to monitor drug effects in small animals (2-5). The attraction of the technique is that it is inexpensive, simple to conduct, gives real-time results, and does not require the handling and disposal of radioactive isotopes. NIR fluorescence penetrates more deeply into tissues because it has lower tissue absorption and scattering of light, and causes relatively little autofluorescence.

It has recently been observed that PS becomes exposed on the outer surface of viable (non-apoptotic) endothelial cells in tumor blood vessels, probably in response to oxidative stresses present in the tumor microenvironment (6, 7). Vascular endothelium in normal tissues lacks exposed PS. Thus, in addition to imaging apoptotic tumor cells, PS binding probes also image the exposed PS on tumor vasculature. We have developed a series of monoclonal antibodies that recognize PS with higher specificity than does annexin V (6, 8, 9). The antibodies bind to PS complexed with the PS-binding protein, β2-glycoprotein I (β2GP1) (9).

In the present study, we used a new, fully human PS targeting antibody, PGN635 (10). We conjugated the F(ab')$_2$ fragment of PGN635 to an NIR dye, IRDye800CW, and used optical imaging to study exposed PS on subcutaneous U87

Reporters, Markers, Dyes, Nanoparticles, and Molecular Probes for Biomedical Applications V,
edited by Samuel Achilefu, Ramesh Raghavachari, Proc. of SPIE Vol. 8596, 859603
 · doi: 10.1117/12.2007291

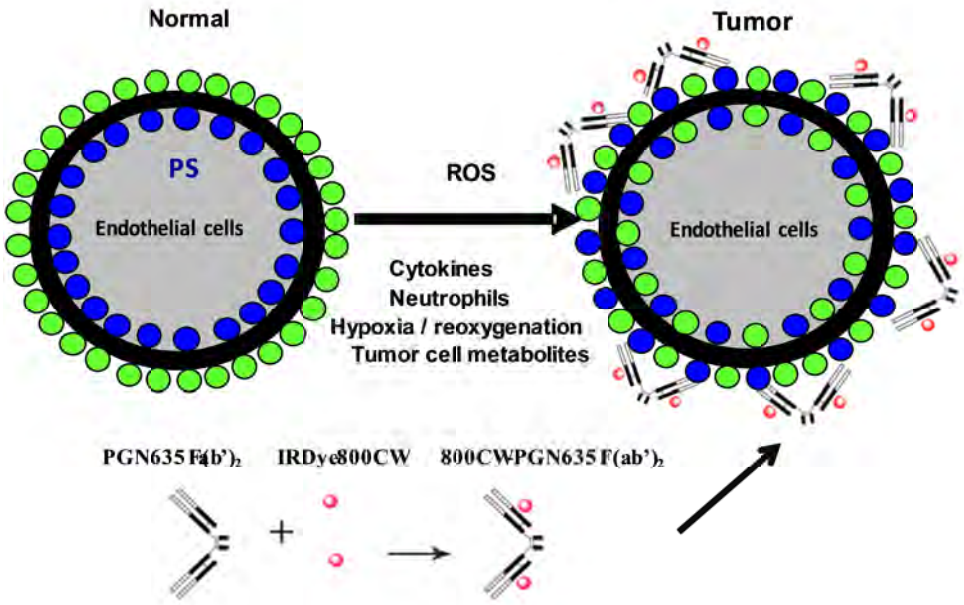
Normal
Tumor
PS
Endothelial cells
ROS
Endothelial cells
Cytokines
Neutrophils
Hypoxia / reoxygenation
Tumor cell metabolites
PGN635F(ab')2
IRDye800CW
800CW-PGN635F(ab')2

reached ~ 5 mm in diameter, 150 μg of PGN635 or the control antibody Aurexis were injected *i.v.* and allowed to circulate for 4 h. The mice were anesthetized, exsanguinated, and perfused with heparinized saline. The tumors were removed and frozen for preparation of cryosections. Vascular endothelium was stained using a rat anti-mouse CD31 antibody (BD Biosciences, San Jose, CA) followed by Cy3-labeled goat anti-rat IgG. PGN635 and Aurexis were detected using biotinylated goat anti-human IgG conjugated to Cy2. Images were captured using a Coolsnap digital camera mounted on a Nikon microscope and analyzed with MetaVue software (Universal Imaging Corporation). Doubly labeled endothelial cells (i.e. CD31 positive/PGN635 positive) were identified by yellow fluorescence on merged images. The percentage of doubly positive vessels was calculated as follows: (mean number of yellow vessels per field/mean number of total vessels) × 100. Ten random 0.079-mm^2 fields were evaluated for each tumor section.

2.4 Near Infrared Fluorescence Imaging

When the subcutaneous tumors reached ~ 5 mm in diameter, *in vivo* fluorescence imaging was performed using a Maestro imaging system (CRI Inc. Woburn, MA). Each mouse was maintained under general anesthesia (air and 2% isoflurane). NIR images were acquired before and at different times after administration of 800CW-PGN635F(ab')$_2$ or 800CW-AurexisF(ab')$_2$ (2 nmol/mouse) via a tail vein. A set of filters specifically for NIR imaging (excitation, 671-705 nm; emission, 730-950 nm) was applied.

Fluorescence images were processed with Maestro software 2.8 (5). A spectrum for background signal (peak emission ~ 770 nm) was first obtained from a mouse before injection of 800CW-antibody F(ab')$_2$. The spectrum of 800CW conjugates (peak emission ~ 800 nm) was obtained from a solution of the dye in PBS. The spectra were then imported and used to unmix the NIR dye signal from the background signal for both *in vivo* and *ex vivo* studies. The whole set of *in vivo* images of each individual mouse, obtained before and at various times after injection of the dye, was examined for quantification. A common ROI was based on the most obvious signal of the tumor 24 h after injection and was applied to both the tumor and normal tissue of each image. Because the intensity of emitted light fade over time, longer exposure times were typically used for the later time points. The total photon counts were normalized by time (counts/s) and identical ROI were compared to detect dynamic changes in signal intensity. These data were used to construct the histograms in the Figures.

2.5 *Ex vivo* fluorescence imaging

Immediately after the last *in vivo* image, tumor-bearing mice were sacrificed and tumor tissues and thigh muscles were dissected. *Ex vivo* fluorescence imaging was performed using the Maestro imaging system.

2.6 Near infrared fluorescence microscopy

Immediately after *in vivo* imaging, tumor-bearing mice were sacrificed and tumor tissues were dissected out. The cryosections were immunostained with antibodies to the endothelial marker, CD31 (Serotec, Raleigh, NC) followed by Cy3-conjugated secondary antibody (Jackson Immunoresearch Laboratories, West Grove, PA). The NIR fluorescence signal was detected using a Zeiss AxioObserver (Carl Zeiss MicroImaging, Inc., Thornwood, NY) equipped with NIR filters. The NIR signals were recorded and merged with the CD31 image and the DAPI-stained image of the same field.

2.7 Statistical analysis

Statistical significance was assessed using an ANOVA on the basis of Fisher's protected least significant difference (PLSD; Statview; SAS Institute Inc., Cary, NC) or Student's t tests.

3. RESULTS

3.1 Detection and quantification of exposed PS in vivo

An average of 27 ± 10 % of blood vessels in U87 tumors had exposed PS on their endothelium, as judged by coincident staining of vessels by PGN635 and anti-CD31 (Fig. 2). For the orthotopic MDA-MB231 breast tumors, an average of PGN635 was 30 ± 8% of the vessels were stained by PGN635. For both tumor types, minimal staining for the control antibody Aurexis was observed (Fig. 2, $p < 0.01$).

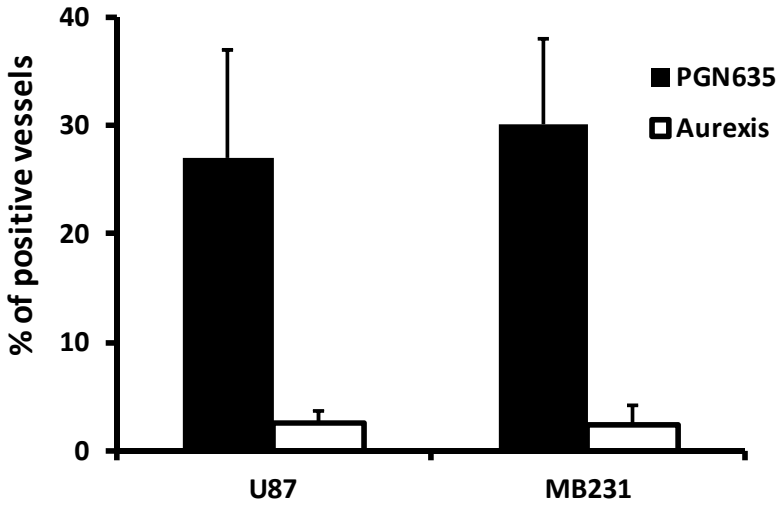

Figure 2. Specificity study of PS-targeting antibody PGN635 co-localized with tumor vascular endothelial cells by immunohistochmical staining. Mice bearing a subcutaneous U87 glioma or orthotopic MDA-MB231 breast cancer were injected intravenously with full length PGN635 or control antibody Aurexis. Animals were sacrificed and perfused with saline 3 h later. Frozen sections of tumor tissues were analyzed for the presence of PGN635 by detecting the PGN635 with fluorescent-labeled human IgG. Vascular endothelial cells were counterstained with anti-CD31. Merged images were used to determine coincidence of staining to confirm that PGN635 was bound to tumor vascular endothelial cells. Staining with PGN635 was antigen-specific since Aurexis gave low levels of staining.

3.2 *In vivo* optical imaging of exposed PS on tumor vascular endothelial cells

In Figure 3 are presented the *in vivo* time course data for 800CW-PGN635F(ab')$_2$, showing it has high selectivity for subcutaneous U87 tumors in mice. Clear contrast between the tumor and contralateral normal tissue was visible 24 h after injection and improved still further by 48 h after injection. Time course studies showed that the light intensity in both the tumor and normal tissue was maximal 5 min after injection, and then decreased abruptly over the next 4 h. However, in contrast to the fast wash out in normal tissues, the signal in the tumor was maintained over time. Tumor/normal ratio (TNR) was 2.9 at 24 h and 3.4 at 48 h. Similar results were obtained for the orthotopic MDA-MB231 breast cancer (TNR = 2.8 at 24 h).

Immediately after *in vivo* optical imaging, *ex vivo* optical imaging was performed on excised tumor and normal muscle. In good agreement with the *in vivo* data, significantly higher optical signal was observed in tumor versus normal muscle ($p < 0.05$). The specificity of PGN635F(ab')$_2$ bound to tumor vasculature was confirmed by fluorescence microscopical studies demonstrating colocalization of 800CW-PGN635F(ab')$_2$ with CD31-positive tumor vascular endothelium.

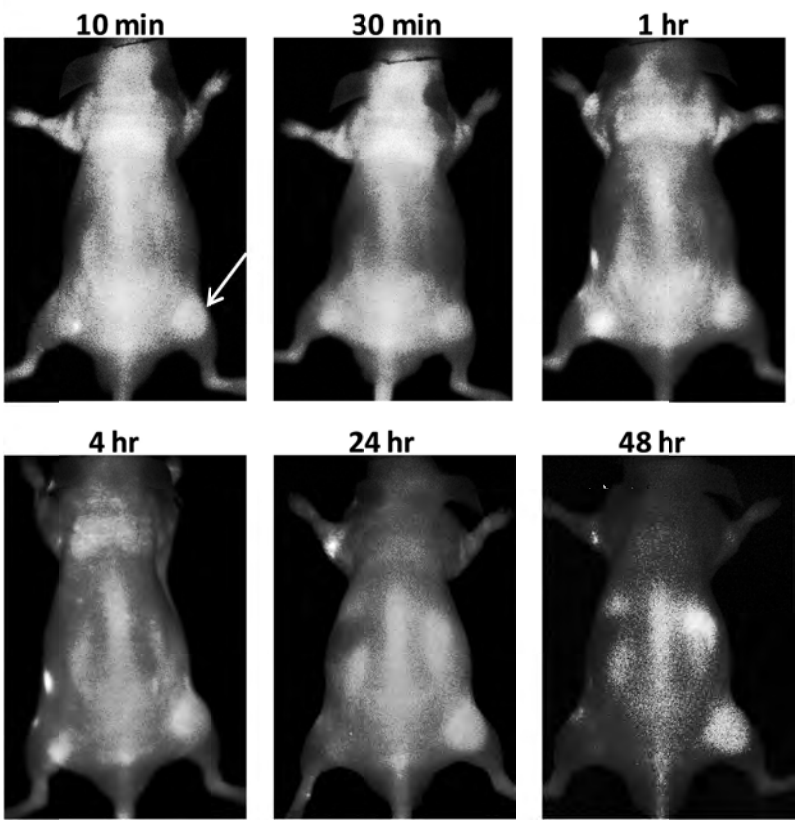
10 min
30 min
1 hr
4 hr
24 hr
48 hr

Clinical applications of optical imaging are currently limited to the detection of tumor margins or deposits during surgery, to the detection of superficial tumors, and to the detection of deep-seated tumors by endoscopy. The current study is also a proof of principle study, indicating the potential of this unique antibody for detecting deep-seated tumors using PET, SPECT, or MRI. Other imaging contrast agents should be considered for attachment to PGN635 $F(ab')_2$ fragments. PGN635 is particularly impressive as a targeting ligand because of its high specificity, lack of uptake by the liver or any other organs, rapid acquisition by its vascular target, and its persistence on the vascular target for days.

5. CONCLUSION

We have previously discovered that PS is exposed specifically on tumor vascular endothelial cells, but not on normal vascular endothelium. In the present study, we have combined NIR optical imaging with the $F(ab')_2$ fragment of PGN635, a novel monoclonal antibody that targets PS, to imaging *in vivo* tumor vasculature of glioma and breast cancer in mouse models. The high tumor specificity of PGN635 underscores the prospect of using PGN635$F(ab')_2$ and related antibodies for imaging tumor vasculature in humans.

ACKNOWLEDGEMENTS

We thank Peregrine Pharmaceuticals Inc., Tustin, CA, for the provision of PGN635 antibody. This work was supported in part by NCI 1R21 CA141348-01A1 and W81XWH-12-1-0317 and by Gillson Longenbaugh Foundation,, TX. Imaging was performed with the CRi Maestro was provided by the Joint Program in BME through a DOE grant #DE-FG02-05CH11280.

REFERENCES

[1]. W. Cai, G. Niu and X. Chen, "Imaging of integrins as biomarkers for tumor angiogenesis," Curr Pharm Des 14(28), 2943-2973 (2008)

[2]. K. E. Adams, S. Ke, S. Kwon, F. Liang, Z. Fan, Y. Lu, K. Hirschi, M. E. Mawad, M. A. Barry and E. M. Sevick-Muraca, "Comparison of visible and near-infrared wavelength-excitable fluorescent dyes for molecular imaging of cancer," J Biomed Opt 12(2), 024017 (2007)

[3]. A. R. Hsu, W. Cai, A. Veeravagu, K. A. Mohamedali, K. Chen, S. Kim, H. Vogel, L. C. Hou, V. Tse, M. G. Rosenblum and X. Chen, "Multimodality molecular imaging of glioblastoma growth inhibition with vasculature-targeting fusion toxin VEGF121/rGel," J Nucl Med 48(3), 445-454 (2007)

[4]. Y. Hama, Y. Urano, Y. Koyama, P. L. Choyke and H. Kobayashi, "Activatable fluorescent molecular imaging of peritoneal metastases following pretargeting with a biotinylated monoclonal antibody," Cancer Res 67(8), 3809-3817 (2007)

[5]. H. Zhou, K. Luby-Phelps, B. E. Mickey, A. A. Habib, R. P. Mason and D. Zhao, "Dynamic near-infrared optical imaging of 2-deoxyglucose uptake by intracranial glioma of athymic mice," PLoS One 4(11), e8051 (2009)

[6]. S. Ran, A. Downes and P. E. Thorpe, "Increased exposure of anionic phospholipids on the surface of tumor blood vessels," Cancer Res 62(21), 6132-6140 (2002)

[7]. S. Ran and P. E. Thorpe, "Phosphatidylserine is a marker of tumor vasculature and a potential target for cancer imaging and therapy," Int J Radiat Oncol Biol Phys 54(5), 1479-1484 (2002)

[8]. S. Ran, J. He, X. Huang, M. Soares, D. Scothorn and P. E. Thorpe, "Antitumor effects of a monoclonal antibody that binds anionic phospholipids on the surface of tumor blood vessels in mice," Clin Cancer Res 11(4), 1551-1562 (2005)

[9]. T. A. Luster, J. He, X. Huang, S. N. Maiti, A. J. Schroit, P. G. de Groot and P. E. Thorpe, "Plasma protein beta-2-glycoprotein 1 mediates interaction between the anti-tumor monoclonal antibody 3G4 and anionic phospholipids on

endothelial cells," J Biol Chem 281(40), 29863-29871 (2006)
[10].D. Zhao, J. H. Stafford, H. Zhou and P. E. Thorpe, "Near-infrared Optical Imaging of Exposed Phosphatidylserine in a Mouse Glioma Model," Transl Oncol 4(6), 355-364 (2011)
[11].K. Balasubramanian and A. J. Schroit, "Aminophospholipid asymmetry: A matter of life and death," Annu Rev Physiol 65(701-734 (2003)
[12].D. E. Gerber, A. T. Stopeck, L. Wong, L. S. Rosen, P. E. Thorpe, J. S. Shan and N. K. Ibrahim, "Phase I safety and pharmacokinetic study of bavituximab, a chimeric phosphatidylserine-targeting monoclonal antibody, in patients with advanced solid tumors," Clin Cancer Res 17(21), 6888-6896
[13].R. G. Blasberg and J. Gelovani, "Molecular-genetic imaging: a nuclear medicine-based perspective," Mol Imaging 1(3), 280-300 (2002)

* Dawen.Zhao@UTSouthwestern.edu; phone 1 214 648-9621; fax 1 214 648-4538; Department of Radiology, UT Southwestern Medical Center at Dallas, 5323 Harry Hines Blvd., Dallas, TX, USA 75390-9058

Phosphatidylserine targeted multimodal imaging of brain metastases in mouse models

Dawen Zhao[1], Heling Zhou[1], Srinivas Chiguru[1], Nikolai Slavine[1], Jason H. Stafford[2], Philip E. Thorpe[2]
Departments of Radiology [1]and Pharmacology[2], UT Southwestern Medical Center, Dallas, TX, USA.

Abstract: Brain metastasis is the most common intracranial malignancy in adults. The prognosis is poor, partly because most patients diagnosed with a solitary cerebral metastasis have undetected lesions, and current systemic therapies have limited access to occult metastases with an impermeable brain-tumor-barrier (BTB). Thus, there is an urgent need to develop new diagnostic and therapeutic agents that specifically target brain metastases. Phosphatidylserine (PS), normally restricted to the inner leaflet of the plasma membrane, becomes exposed on the outer surface of viable (non-apoptotic) endothelial cells in tumor vasculature. Vascular endothelium in normal tissues does not have exposed PS. In this study, we used a fully human monoclonal antibody, PGN635, that targets PS to identify brain metastases in mouse models. Brain-tropic human breast cancer MDA-MB-231/BR-GFP (231-Br) or mouse breast tumor 4T1 cells were injected directly into the left ventricle of a mouse heart under the imaging guidance of a small animal ultrasound machine. Multifocal lesions developed in the 231-Br mouse brain, while a solitary brain tumor was seen in 4T1 model by MRI scans. Fluorescence microscopy of sections of brain showed that there is extensive PS exposure (93 ± 5%) on vascular endothelial cells in the brain metastases but not in normal brain. *Ex vivo* imaging at 24 h post *i.v.* injection of PGN635F(ab')$_2$ labeled with near infrared dye, IRDye800CW, allowed clear visualization not only of a single deep-seated 4T1 tumor (TNR = 5.8), but also individual brain metastases of 231-Br (TNR = 3.1). We have further exploited I-124 labeled PGN635F(ab')$_2$ for *in vivo* PET imaging of brain metastases in the 231-Br model. PET/CT images were acquired 24 h and 48 h later. PET/CT merged images at 48 h showed a complete absence of uptake by the normal mouse brain. In contrast, multiple sites of localized uptake were observed in brains bearing metastases, indicating the uptake of I-124-PGN635F(ab')$_2$ by the metastatic lesions. Specificity of PGN635 to brain metastases was further confirmed by *ex vivo* autoradiography. There was also spatial correlation between tumor lesions on MRI and the hot spots on the autoradiograph. Our study suggests that PS appears to be an excellent marker for the development of imaging and targeted therapeutics for brain metastases.

Acknowledgments: We thank Peregrine Pharmaceuticals Inc., Tustin, CA, for the provision of PGN635 antibody. This work was supported in part by DOD W81XWH-08-1-0583, DOD W81XWH-12-1-0317 and by the Meredith D. Chesler Foundation, Dallas, TX. Imaging was conducted by DOE grant #DE-FG02-05CH11280 and NIH BTRP # P41-RR02584.

In vivo MRI and optical imaging of tumor vascular endothelial cells using bimodal liposomal nanoparticles

Liang Zhang[1], Heling Zhou[1], Philip E. Thorpe[2], Dawen Zhao[1]

Departments of Radiology [1] and Pharmacology[2], UT Southwestern Medical Center, Dallas, TX, USA.

Abstract: Phosphatidylserine (PS), normally restricted to the inner leaflet of the plasma membrane, becomes exposed on the outer surface of viable (non-apoptotic) endothelial cells in tumor vasculature, but not in normal blood vessels. In the present study, we report the use of *in vivo* molecular MRI/optical imaging to detect exposed PS on tumor vasculature based on a novel human monoclonal antibody, PGN635 that specifically targets PS. The $F(ab')_2$ fragments of PGN635 were conjugated to polyethylene glycol (PEG)-coated liposomes. MR contrast, paramagnetic iron oxide nanoparticles (IO) were packed into the hydrophilic core of liposome, while near infrared dye, DiR was incorporated into the lipophilic bilayer. Specificity of the dual contrast liposomes (100 nm hydrodynamic diameter) bound to PS-exposed vascular endothelial cells was first studied by *in vitro* histological staining and MRI/optical imaging. At 9.4T MRI, significant reductions in T_2-weighted signal intensity and T_2 values were detected in cultured vascular endothelial cells treated with irradiation (6 Gy; $p < 0.05$), while no change was observed in nonirradiated cells, or in irradiated cells treated with control antibody conjugates or pretreated with PGN635 antibodies (blocking study). Similar results were observed by fluorescence microscopy. *In vivo* longitudinal MRI and optical imaging were performed after *i.v.* injection of the dual contrast liposomes into mice bearing subcutaneous breast MDA-MB231 tumors. NIR optical imaging revealed a clear tumor contrast in non-irradiated tumors 24 h later (tumor/normal ratio (TNR) = 3.8 ± 0.6). Irradiation significantly increased PS exposure on tumor vascular endothelial cells, resulting an enhanced tumor contrast at 24 h (TNR = 5.2 ± 0.9). At 9.4 T MRI, longitudinal T_2-weighted images detected inhomogeneous signal loss in tumor at 24 h (mean TNR decrease = 15 ± 3%). Irradiation treated tumors showed significantly more hypointense regions (mean TNR decrease = 47 ± 6%; $p < 0.01$). The vascular location of IO-DiR-PGN635$F(ab')_2$ liposomes was confirmed by Prussian blue staining and immunohistochemical staining of CD31-positive blood vessels. Localization of IO-DiR-PGN635 $F(ab')_2$ liposomes to tumor blood vessels was antigen specific, since IO-DiR-Aurexis $F(ab')_2$, a control probe of irrelevant specificity, showed minimal accumulation in the tumors. Our studies suggest that tumor vasculature can be successfully imaged *in vivo* with molecular imaging modalities to provide sensitive tumor detection.

Acknowledgments: We thank Peregrine Pharmaceuticals Inc., Tustin, CA, for the provision of PGN635 antibody. This work was supported in part by DOD W81XWH-12-1-0317 and by the Gillson Longenbaugh Foundation, Dallas, TX. Imaging was conducted by DOE grant #DE-FG02-05CH11280 and NIH BTRP # P41-RR02584.

Ultrasound imaging-guided intracardiac injection to develop a mouse model of breast cancer brain metastases followed by longitudinal MRI

Heling Zhou and Dawen Zhao

Authors: institution(s)/affiliation(s) for each author:

Heling Zhou, PhD
Radiology
University of Texas Southwestern Medical Center
Heling.Zhou@UTSouthwestern.edu

Dawen Zhao, MD, PhD
Radiology
University of Texas Southwestern Medical Center
Dawen.Zhao@UTSouthwestern.edu

Corresponding author: Dawen Zhao

Key words: breast cancer brain metastasis, ultrasound imaging, intracardiac injection, MRI

Short abstract:
A breast cancer brain metastasis mouse model is established with ultrasound imaging-guided intracardiac injection of MDA-MB231Br-GFP cells. Development of multifocal intracranial metastases has been monitored longitudinally using high-resolution 9.4T MRI.

Long abstract:
Breast cancer brain metastasis, occurring in 30% of breast cancer patients at stage IV, is associated with high mortality. The median survival is only 6 months. It is critical to have suitable animal models to mimic the hemodynamic spread of the metastatic cells in the clinical scenario. Here, we are introducing the use of small animal ultrasound imaging to guide an accurate injection of brain tropical breast cancer cells into the left ventricle of athymic nude mice. Longitudinal MRI is used to assessing intracranial initiation and growth of brain metastases. Ultrasound-guided intracardiac injection ensures not only an accurate injection and hereby a higher successful rate but also significantly decreased mortality rate, as compared to our previous manual procedure. *In vivo* high resolution MRI allows the visualization of hyperintense multi-focal lesions, as small as 310 μm in diameter on T_2-weighted images at 3 weeks post injection. Follow-up MRI reveals intracranial tumor growth and increased number of metastases that distribute throughout the whole brain.

Introduction:
Brain metastasis is the most common intracranial malignancy in adults. The prognosis is extremely poor, with a median survival of 4-6 months even with aggressive treatment. Breast cancer is one of the three major primary cancers with a high morbidity of brain metastasis [1-3]. Several brain-tropic breast cancer lines are capable of developing brain metastases after intracardiac or intracarotid injection[4]. The MDA-MB231Br line is one of the most widely used human breast cancer lines to develop brain metastasis in rodent models[5,6].

Like many other studies[4,7], we have performed a manual procedure of intracardiac injection in our previous studies. However, only 50% successful rate was obtained with the manual injection and a fraction of mice died from the repeated invasive procedures if prior trials failed. Here, we are introducing the use of an imaging-guided procedure to secure the injection of brain-seeking breast cancer cells into the left ventricle of athymic mice. Longitudinal high resolution MRI is applied to follow intracranial development of brain metastases.

Protocol Text:

All animal procedures were approved by the Institutional Animal Care and Use Committee of University of Texas Southwestern Medical Center.

1) Preparation of the MDA-MB231/Br-GFP cells

1.1) Retrieve and culture the MDA-MB231/Br-GFP cells (kindly provided by Drs. Palmieri and Steeg, NCI) in DMEM medium containing 10% FBS, 1% glutamine and 1% penicillin/streptomycin.

1.2) Oberserving the condition of the cells and color of medium, and replace medium every 2-3 days.

1.3) Tripsinize and collect the cells when 80% confluence is reached.

1.3.1) Remove the old medium completely and add 5ml PBS (x1) to wash the cells gently. Remove the PBS from the dish.

1.3.2) Add 1.5ml Typsin in the dish, tilt the dish gently to ensure all the cells are covered by Typsin.

1.3.3) Put the dish back to the cell incubator and keep it at 37°C for 1 minute.

1.3.4) Take the dish out of incubator and observe the cells under optical microscope to ensure the cells detach from the dish.

1.3.5) Add 3ml medium to stop the effect of trypsin. Collect the cell mixture in a centrifuge tube.

1.3.6) Centrifuge the mixture at 2000 r/min for 5 minutes.

1.3.7) Remove the medium carefully and resuspend the cells in 5 ml serum free medium homogeniously.

1.4) Count appropriate number of cells and resuspend them in serum free DEME medium with a final concentration of $1.75x10^5$ cells in 100 µl volume.

1.4.1) Take 50µl cell mixture and add 50µl Trypan Blue. After mixing, take 10µl mixture and carefully add to the cell counting slide. Use multiple samples to ensure accurate cell number estimation.

1.4.2) Stick in the cell counting slide, one end at a time and the cell counter starts counting automatically. Take average of all the counting results and calculate the total cell number.

1.4.3) Centrifuge the cells again and resuspend them in the appropriate volume of serum free medium to result in the final concentration of $1.75x10^5$ cells per 100 µl volume.

1.5) Place cells on ice prior to intracardiac injection.

2) Ultrasound imaging-guided intracardicac injection

2.1) Female nude mice (BALB/c nu/nu) at 6-8 weeks old are used in this study.

2.2) Ultrasound imaging is performed on a VisualSonics Vevo 770 High-Resolution Imaging System.

2.3) Log in the imaging system. Initialize the transducer 704 (40MHz).

2.4) Start a new study and fill in the information.

2.5) Anesthetize (3% isoflurane/100% O_2 in an induction chamber) and maintain the animals with isoflurane (2%) in 100% O_2 (1 dm^3/min) during the surgical procedure via a nose cone.

2.6) Set the temperature of the imaging table to 37 °C. Tape the anesthetized mouse to the heated imaging table in supine position.

2.7) Keep the ultrasound gel at 37 °C prior to imaging. Apply the gel to the chest of the mouse.

2.8) Mount the transducer in the holder. Lower the transducer till the desired imaging depth is reached. Move the stage until the left ventricle is identified with the ascending aorta as the landmark (Figure 1A). Lock the stage when a clear view of left ventricle is visualized.

2.9) Draw 100µl of cell mixture into a 1 ml syringe with a 22 G needle. Place and fix the syringe on the syringe mount.

2.10) Move the syringe forward towards the mouse chest and carefully move it side to side until the needle tip is in the imaging field of view (before entering the mouse).

2.11) Adjust the needle height and angle to aim down the left ventricle.

2.12) Penetrate the syringe needle promptly through skin and muscle layers into the left ventricle under the guidance of ultrasound imaging.

An indication of successful insertion of the needle into the left ventricle is the reflux of fresh arterial blood (pink color in contrast to dark red venous blood) into the syringe

2.13) Inject the cell mixture slowly (Figure 1B).

2.14) Upon completion, withdraw the needle, lift up the transducer, clean the ultrasound gel with dampened gauze and remove tape

2.15) Prepare a clean cage with a preheated pad.

2.16) Place the animal on the pad and observe the animal till full recovery.

2.17) Monitor the behavior of the animal every 24 hours for two days.

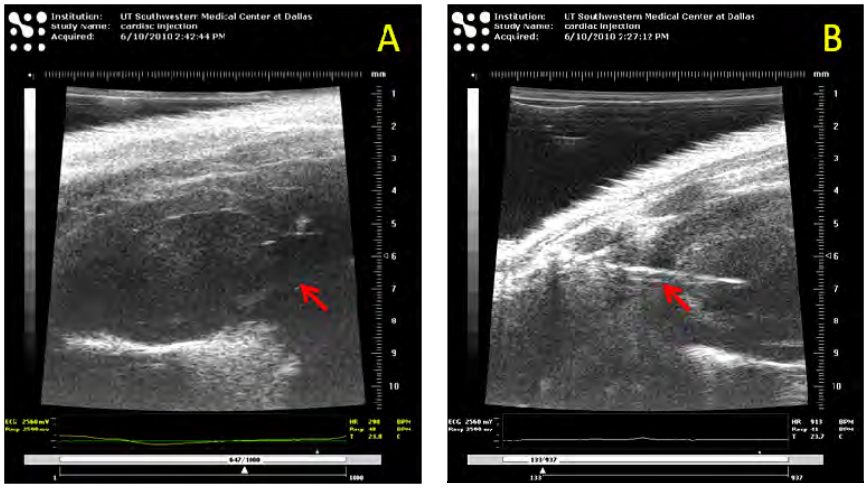

Figure 1 Ultrasound-guided intracardiac injection.

(A) Identification of the ascending aorta (arrow) as the landmark of left ventricle of the mouse heart. (B) A needle (arrow) insertion into the left ventricle to inject the tumor cells.

3) MRI monitoring of intracranial tumor development

3.1) A 9.4 Tesla horizontal bore magnet with a Varian INOVA Unity system is used to monitoring intracranial development of brain metastases.

3.2) MRI is initiated two weeks after tumor implantation and repeated once a week for up to three weeks.

3.3) Sedate the animals with 3% isoflurane and maintain them under general anesthesia (1.5% isoflurane).

3.4) Monitor and maintain the animal body temperature and respiration constant throughout the experiment.

3.5) High resolution multi-slice (14 slices with 1mm-thick, no gap) T_1- and T_2-weighted coronal images, covering the region from the frontal lobe to the posterior fossa, are acquired with the following parameters: T_1-weighted images: spin echo multiple slice (SEMS), TR/TE = 400 ms/20 ms, matrix: 256 x 256, FOV 20 x 20 mm, in plane resolution: 78 x 78 μm^2. T_2-weighted images: fast spin echo multiple slice (FSEMS) sequences, TR/TE = 2500 ms/48 ms, 8 echo trains, matrix: 256 x 256, FOV 20 x 20 mm, in plane resolution: 78 x 78 μm^2 [8,9].

Tumor lesions appear brighter than normal brain tissues on T_2-weighted images.

3.6) Tumor size is determined on T_2-weighted images by manually outlining the enhancing portion of the mass on each image by using MatLab programs written by us[8].

Given most of the tumor diameters are smaller than the slice thickness (1 mm), the tumor size is presented as in plane area rather than the volume.

4) H&E staining confirming the metastases

4.1) Sacrifice the mice immediately after the last MR scan, dissect the tumor-bearing brains and embed it in O.C.T medium and frozen in -80 ºC.

4.2) Section a series of 10 μm-thick coronal brain specimens with cryostat.

4.3) Perform H&E staining on the brain sections.

Representative Results

With the high spatial resolution of MRI (78 μm in plane resolution), hyperintense lesions can be identified as small as 310 μm in diameter (Fig. 2). Since the metastases in this study are very small and development of necrosis and edema is minimal, the hyperintense lesion on T_2-weighted images truly represented the tumor mass.

Longitudinal MRI studies allow *in vivo* non-invasive evaluation of tumor growth. As shown in figure 3, the high resolution MRI was able to detect several small lesions 3 weeks after intracardiac injection (Fig. 3A). On week 4, the lesions that were seen in the previous scan all became larger; more new lesions appeared on T_2-weighted images (Fig. 3B).

H&E staining revealed either diffuse or cluster type metastatic lesions (Fig. 4). Enlarged vessels were often seen around the tumor, indicating non-sprouting angiogenesis (Fig. 4D).

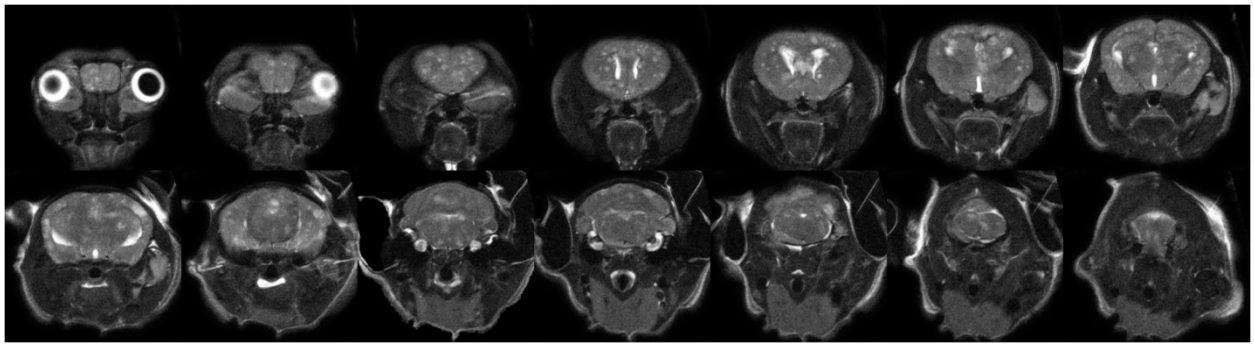

Figure 2. High resolution T_2-weighted images of breast cancer brain metastases. Fourteen consecutive MRI slices of a representative mouse brain, acquired four weeks after intracardiac injection, clearly revealed the multifocal metastases distributing through the whole mouse brain, from olfactory bulb to pontine and medulla.

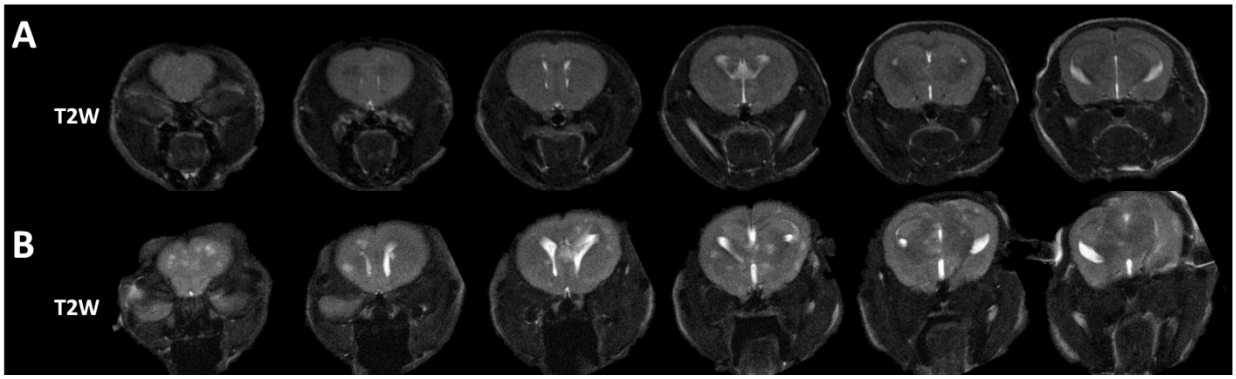

Figure 3. Longitudinal MRI of development of brain metastases.
A. Six consecutive coronal MRI sections at week 3 identified multiple lesions with hyper-intensity on T_2-weighted images. B. An increased number of lesions appeared on the images at week 4, and those lesions seen on week 3 became larger.

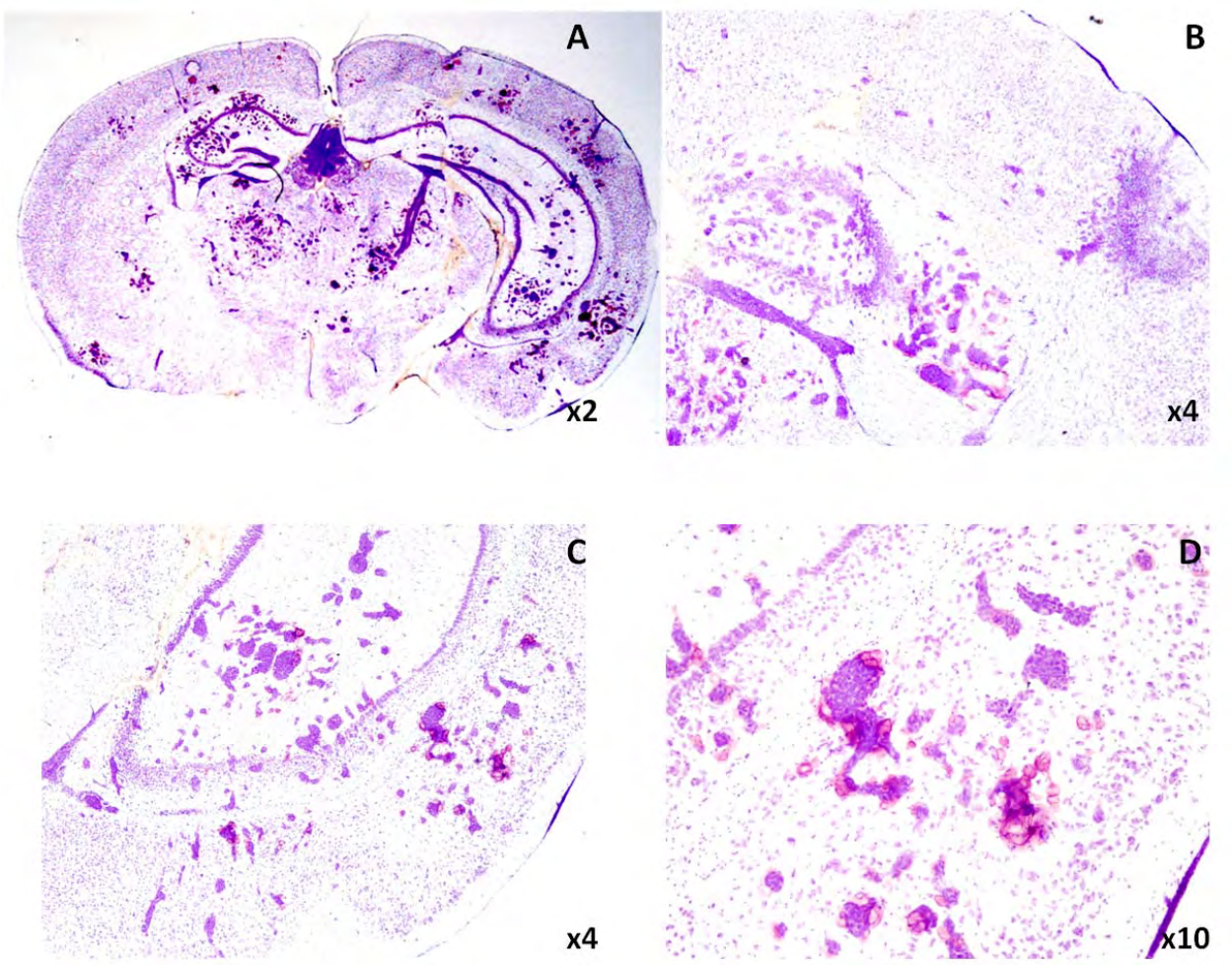

Figure 4. Microscopic lesions were observed on H&E staining.
A. A whole mount coronal section depicted multiple lesions. B-D. Higher magnification images showed either diffuse or cluster type lesions (B and C). Enlarged vessels were seen around the tumor.

Discussion

In the present study, we have demonstrated that ultrasound imaging-guided left ventricular injection ensures the accuracy so that every animal in this study developed brain metastases and no animal death was observed.

Current understandings of intracranial development of brain metastases are largely based on histological studies on animal models [4,10]. However, histological studies normally require a large number of mice that are killed at different time points after tumor implantation. More importantly, information about temporal development in individual lesions is lacking from histological studies.

In vivo imaging promises greater efficiency since each animal serves as its own control and multiple time points can be examined sequentially[7,11]. High resolution T_2-weighted images enable the detection of multifocal tumor initiation at very early stage (lesions with diameter as small as 310 μm are visible). Longitudinal MRI allows individual brain metastases to be examined over time. Moreover, *in vivo* non-invasive MRI will be particularly valuable in longitudinal study of therapeutic response, *e.g.*, whole brain radiation.

Formation of multi-focal brain metastases is the characteristics of the MDA-MB231Br model. In contrast, several other brain-seeking lines such as MCF-7Br and 4T1 have been shown to develop a solitary metastasis after intracardiac injection[12]. Both of the models, mirroring clinical counterparts, are useful animal models of brain metastasis. However, in addition to brain metastases, visceral metastases, such as lung and bone metastases are often observed in this model. Establishment of animal models that develop brain metastases exclusively will be critical, in particular, for evaluation of treatment response.

In conclusion, we have demonstrated the usefulness of imaging-guided intracardiac injection to establish a brain metastasis mouse model and the high resolution MRI to assess intracranial development of multi-focal metastases in a mouse model.

Acknowledgements:

We are grateful to Drs. Diane Palmieri and Patricia Steeg of NCI for providing us MDA-MB231Br cells. We thank Dr. Ralph Mason, Mr. Jason Reneau and Ms. Ramona Lopes for technical and collegial support.This work was supported in part by the DOD IDEA Awards W81XWH-08-1-0583 and W81XWH-12-1-0317. MRI experiments were performed in the Advanced Imaging Research Center, an NIH BTRP # P41-RR02584 facility, and ultrasound-guided intracardiac injection was performed with VisualSonics Vevo 770 under 1S10RR02564801.

Disclosures: No conflicts of interest declared.

Table of specific reagents and equipments:

Name of the reagent or equipment	Company	Catalogue number	Comments (optional)
DMEM	HyClone	SH30022.01	
Trypsin	Mediatech	25-051-C1	
Automatic cell counter	Biorad	TC10	
Isoflurane	Baxter International Inc.	1001936060	
VisualSonics Vevo	Visual Sonics Inc.		

770 High-Resolution Imaging System			
9.4T horizontal bore magnet with a Varian INOVA Unity system	Agilent		
O.C.T Compound	Sakura Finetek USA	4583	

References

1 Schouten, L. J. *et al.* Incidence of brain metastases in a cohort of patients with carcinoma of the breast, colon, kidney, and lung and melanoma. *Cancer* **94**, 2698-2705 (2002).

2 Lin, N. U. *et al.* CNS metastases in breast cancer. *J Clin Oncol* **22**, 3608-3617, doi:10.1200/JCO.2004.01.175 22/17/3608 [pii] (2004).

3 Eichler, A. F. *et al.* The biology of brain metastases-translation to new therapies. *Nat Rev Clin Oncol*, doi:nrclinonc.2011.58 [pii] 10.1038/nrclinonc.2011.58 (2011).

4 Lockman, P. R. *et al.* Heterogeneous blood-tumor barrier permeability determines drug efficacy in experimental brain metastases of breast cancer. *Clin Cancer Res* **16**, 5664-5678, doi:1078-0432.CCR-10-1564 [pii] 10.1158/1078-0432.CCR-10-1564 (2010).

5 Yoneda, T. *et al.* A bone-seeking clone exhibits different biological properties from the MDA-MB-231 parental human breast cancer cells and a brain-seeking clone in vivo and in vitro. *J Bone Miner Res* **16**, 1486-1495 (2001).

6 Palmieri, D. *et al.* Her-2 overexpression increases the metastatic outgrowth of breast cancer cells in the brain. *Cancer Res* **67**, 4190-4198, doi:67/9/4190 [pii] 10.1158/0008-5472.CAN-06-3316 (2007).

7 Percy, D. B. *et al.* In vivo characterization of changing blood-tumor barrier permeability in a mouse model of breast cancer metastasis: a complementary magnetic resonance imaging approach. *Invest Radiol* **46**, 718-725, doi:10.1097/RLI.0b013e318226c427 (2011).

8 Zhou, H. *et al.* Longitudinal MRI evaluation of intracranial development and vascular characteristics of breast cancer brain metastases in a mouse model. *PLoS One* **8** e62238, doi:10.1371/journal.pone.0062238 (2013).

9 Zhou, H. *et al.* Dynamic near-infrared optical imaging of 2-deoxyglucose uptake by intracranial glioma of athymic mice. *PLoS One* **4**, e8051, doi:10.1371/journal.pone.0008051 (2009).

10 Zhang, R. D. *et al.* Differential permeability of the blood-brain barrier in experimental brain metastases produced by human neoplasms implanted into nude mice. *Am J Pathol* **141**, 1115-1124 (1992).

11 Mason, R. P. *et al.* Tumor oximetry: comparison of 19F MR EPI and electrodes. *Adv Exp Med Biol* **530**, 19-27 (2003).

12 Gril, B. *et al.* Pazopanib reveals a role for tumor cell B-Raf in the prevention of HER2+ breast cancer brain metastasis. *Clin Cancer Res* **17**, 142-153, doi:1078-0432.CCR-10-1603 [pii] 10.1158/1078-0432.CCR-10-1603 (2010).